Reactive Uptake of $ClNO_2$ on Aqueous Bromide Solutions

S. Fickert, F. Helleis, J. W. Adams, G. K. Moortgat, and J. N. Crowley*

Max-Planck-Institut für Chemistry, Division of Atmospheric Chemistry, Postfach 3060, 55020 Mainz, Germany

Received: July 14, 1998; In Final Form: October 7, 1998

The reactive uptake of $ClNO_2$ on pure water, NaBr, and mixed NaBr/NaCl solutions was studied using a wetted wall flow tube equipped with a quadrupole mass spectrometer. The measured uptake coefficient, γ_{expt}, varied between approximately 1×10^{-5} and 1×10^{-4}, depending on the aqueous salt concentration. Parameters governing the reactive uptake on NaBr solutions were determined interdependently as $H^2D_1k_{Br}^{II} = (0.101 \pm 0.015)$ M cm^2 atm^{-2} s^{-2}. The accommodation coefficient, α, for $ClNO_2$ on aqueous solutions at 275 K was found to be $(9 \pm 4) \times 10^{-3}$. The major gas-phase products of the uptake and reaction of $ClNO_2$ and Br^- were found to be Br_2 and $BrNO_2$. $BrNO_2$ is formed initially and is converted to Br_2 in a secondary reaction with Br^- in the aqueous phase. BrCl is a minor product. The presence of 1M Cl^- had no effect on either the kinetics of uptake or the products formed. By exchanging the halide solutions for 0.1 M OH^-, the uptake rate could be increased so that the diffusion limit was reached in the reactor. Variation of the pressure yielded the diffusion coefficients of $ClNO_2$ in He and N_2 as 275 ± 26 and 75 ± 6 Torr cm^2 s^{-1}, respectively. The implications of these results for the halogen chemistry of the marine boundary layer are discussed.

1. Introduction

The presence of reactive halogen species in the marine boundary layer (MBL) at mid-latitudes has been documented by a number of recent field studies. Reactive (photolabile) chlorine species such as HOCl and Cl_2 have been detected in polluted air advecting over the ocean,[1] and the presence of Cl atoms has been inferred from nonmethane-hydrocarbon (NMHC) reactivity patterns in polluted air masses over the North Atlantic[2] and in the remote central Pacific.[3] The calculated concentration of Cl atoms that are formed from reactive chlorine molecules is often sufficient to contribute significantly to the oxidation of many trace gases, especially NMHC. Sea-spray constitutes the largest reservoir of chlorine in the atmosphere, but the mechanism by which it can be released from the aqueous aerosol into the gas phase is not clear. Acid displacement, whereby strong inorganic acids such as HNO_3 or H_2SO_4 liberate chlorine in the form of HCl, can result in a chloride deficit of up to 90% in polluted air masses.[4] However, this does not explain the presence of high concentrations of reactive chlorine, as the HCl released is only slowly converted to Cl atoms via reaction with OH:

$$OH + HCl \rightarrow Cl + H_2O \qquad (R1)$$

Other mechanisms have been proposed that involve heterogeneous reactions of members of the NO_X/NOy families with sea-salt aerosol, in which photolabile chlorine containing species are generated:[5,6]

$$2NO_2 + NaCl \rightarrow NOCl + \text{other products} \qquad (R2)$$

$$N_2O_5 + NaCl \rightarrow ClNO_2 + \text{other products} \qquad (R3)$$

The severe episodic depletion of ozone in the lower Arctic troposphere is now known to be mediated by the presence of reactive bromine compounds. Bromine atom concentrations of up to 1×10^7 cm^{-3} have been inferred from measured NMHC depletion rates,[7,8] and the BrO radical has been measured directly at concentrations of up to 30 pptv.[9−11] The source of reactive bromine is a matter of topical debate though it has become clear that heterogeneous processing by aerosol particles or on the ice or snowpack is necessary to both release bromine and to maintain high gas-phase concentrations.[12−15]

In the present study we evaluate a possible mechanism for the release of both chlorine and bromine containing photolabile compounds from sea-salt aerosol by investigating the uptake and reaction of $ClNO_2$. $ClNO_2$ is formed at yields >90% by reaction of N_2O_5 on aqueous chloride solutions[6] as well as on dry/humidified NaCl surfaces.[5,16]

2. Experimental Method

2.1. Flow Reactor. The uptake and reaction of $ClNO_2$ on Br^-, Cl^-, and OH^- solutions was investigated using a wetted wall flow tube combined with a differentially pumped quadrupole mass spectrometer. The flow tube (Figure 1) consists of a vertically mounted Pyrex glass tube with a thermostated jacket to control the temperature of the aqueous film flowing down the inner wall of the reactor. The internal diameter of the tube is 1.55 cm, the overall length is 35 cm. Aqueous solutions of NaBr and NaCl are transported via a peristaltic pump into a reservoir at the top of the tube, where the upper 10 cm section is separated from the reaction zone by a ground glass piece which is partially plugged by a glass cone with vertical grooves that allow the solution to enter the reactor. This method allowed the flow speed of the film to be regulated by varying the height of the water column above the cone, as well as by exchanging cones with grooves of different depths. A second peristaltic pump was connected to the bottom of the tube to remove the liquid from the reactor. To obtain a uniformly covered glass surface, occasional cleaning of the tube with a mixture of deionized water, 2-propanol, and potassium hydroxide followed by thorough rinsing with deionized water was necessary.

* Author to whom correspondence should be addressed.

10.1021/jp983004n CCC: $15.00
Published on Web 12/04/1998

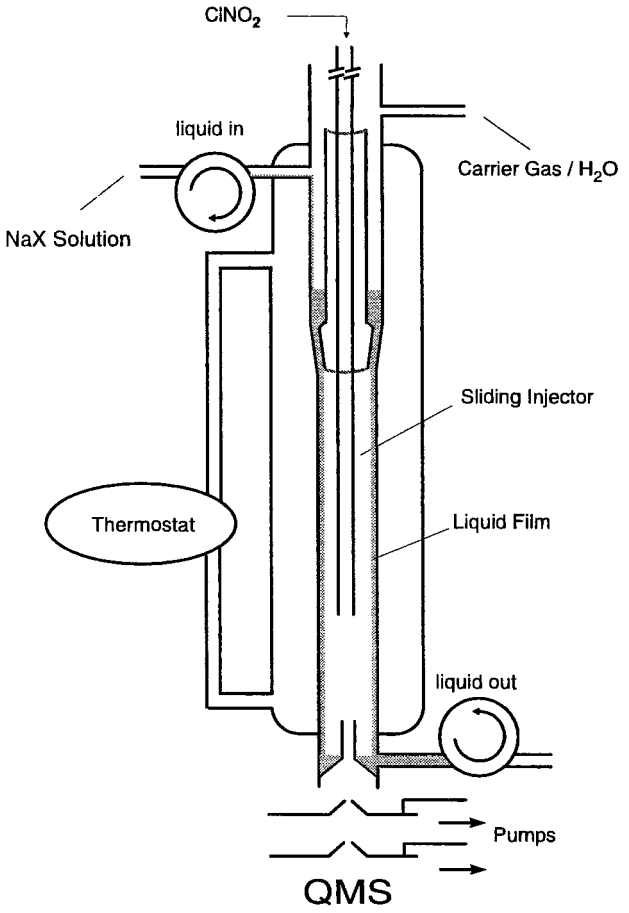

Figure 1. Schematic representation of the wetted wall flow tube experiment. QMS = quadrupole mass spectrometer.

Reactive trace gases, diluted in He, were introduced into the flow tube via a stepper motor driven injector, the translation of which enabled the contact time between trace gas and surface to be varied. The major part of the humidified carrier gas flow was supplied through a side arm of the reactor. Flow rates were obtained by determining the pressure drop, dP/dt, in a calibrated volume. The pressure inside the reactor was measured through a 1/8 in. Teflon tube that led from a 100 Torr (1 Torr = 133.32 Pa) capacitance manometer to the bottom end of the injector. The minimum pressure attainable in our experiments was limited by the vapor pressure of the aqueous solution to ca. 10 Torr. The maximum pressure was determined by the size of the skimmer on the differential pumping system and was ca. 28 Torr for the present experiment.

The resulting molecular beam was modulated at 213 Hz, and gas was analyzed with a quadrupole mass spectrometer (QMS), equipped with an electron-impact ion source. For the conversion of spectrometer signals to absolute concentrations, the QMS was calibrated for all reactants and products involved. In addition, a constant flow of a Kr−Xe mixture (ca. 1×10^{-4} sccm) was added to supply internal standards with the carrier gas in order that corrections for changes of sensitivity could be made. $ClNO_2$ signals were recorded at 49 amu (ClN^+); the characteristic peaks for products were at 93 and 95 amu for $BrNO_2$ ($^{79}BrN^+$ and $^{81}BrN^+$), 96 amu for HOBr, 116 amu for BrCl, and 158 amu for Br_2. The sensitivity of our measurements was reduced by the fact that the nitryl halides were monitored using BrN^+ and ClN^+—the only specific fragments available − instead of NO_2^+, which was about 2 orders of magnitude more abundant.

Liquid samples were analyzed by ion chromatography using a Dionex AS 11 chromatographic column and a conductivity detector. A 5 mM NaOH solution at 1 mL/min was used as eluent under standard conditions.

2.2. Chemicals. All dry chemicals used in the present experiments were analytical grade. Br_2 (> 99.5%, Aldrich) and Cl_2 (> 99.8%, Linde) were used without further purification and diluted to ca. 1 % in He (99.999%, Linde). BrCl was prepared by mixing 3.8 Torr of Br_2 with 3.8 Torr of Cl_2, both diluted in He. The equilibrium concentration of BrCl was determined to an accuracy of ± 5% by UV-absorption spectroscopy.[17] $ClNO_2$ was synthesized according to Volpe et al.[18] by passing a slow stream of HCl (> 99.6%, Linde) and He through a mixture of 100 mL of concentrated H_2SO_4 (95−97%, Merck), 50 mL of fuming H_2SO_4 (ca. 20% free SO_3, Aldrich), and 30 mL of HNO_3 (90%, Aldrich). During the reaction, the mixture was cooled to 273 K. The pale yellow liquid obtained was trapped in liquid nitrogen and transferred into a bubbler where it was stored at 195 K. Gas-phase IR spectra were taken to characterize the product and to check for contaminants. Contributions of NO_2 to the spectrum—presumably from decomposition of $ClNO_2$—were barely discernible, and we set an upper limit of 1% impurity. The vapor pressure of $ClNO_2$ at 195 K was measured to be 18 Torr, and its Cl_2 content (determined by QMS) was less than 5%. A flow of $ClNO_2$ was introduced into the reactor by flowing He through the bubbler held at 195 K and at constant pressure.

2.3. Characterization of the Liquid Film. The salt solutions covering the walls of the tube contained 10^{-4}−10^{-2} M Br^- and in some experiments, 1 M Cl^- also. The thickness of the liquid film, d (cm), and its velocity, v (cm s^{-1}), can be estimated using eq 1:[19]

$$d = 3\sqrt{\frac{3\eta V}{\pi g D \rho}} \tag{1}$$

where η is the viscosity of the liquid (1.89×10^{-2} g cm^{-1} s^{-1} for seawater), V is the liquid flow rate (cm^3 s^{-1}), g is the gravitational acceleration (981 cm s^{-2}), D is the diameter of the tube (1.55 cm), and ρ is the density of the liquid (1.0 g cm^{-3}). For a typical flow rate of 0.1 cm^3 s^{-1}, the film was ≈100 μm thick. Its maximum velocity, v_{max}, at the surface was calculated with eq 2 to be about 3 cm s^{-1}:

$$v_{max} = \frac{3}{2}\left(\frac{V}{\pi D}\right)^{2/3}\left(\frac{\rho g}{3\eta}\right)^{1/3} \tag{2}$$

The Reynold's number of the aqueous film was calculated, as described by Utter et al.,[20] to be 4; i.e., the flow is expected to be laminar, with a smooth velocity gradient across the diameter of the film. Visual inspection confirmed the absence of rippling.

2.4. Characterization of the Gas Flow. For the present experiments, the flow tube reactor was operated in two different regimes. Measurements of diffusion coefficients were performed at flow rates of 200−500 cm^3 STD min^{-1} (sccm) at carrier gas velocities of 100−500 cm s^{-1}, uptake and product studies at ca. 50 cm s^{-1}. Typical pressures ranged from 10 to 28 Torr in both types of experiments. To minimize the influence of gas-phase diffusion on the measured uptake rates, the halide solutions were cooled to 274 K, where their vapor pressures were 4.9 ± 0.2 Torr. For pure Br^- solutions of concentrations up to 10^{-2} M, the vapor pressures are not significantly affected by the presence of salts.[21] Evaporative cooling of the liquid film was avoided by humidifying the main flow of He by passage through a thermostated water bubbler before entering the reactor.

Because of condensation problems, no water was added to the He flux transporting the trace gases through the injector. For this reason, the ratio of $He_{injector}/He_{main}$ was kept as low as possible in all experiments, with a maximum of 30% of nonhumidified carrier gas entering through the injector. Control measurements with a thermocouple inside the reactor showed no significant temperature gradient along the tube. Additionally, for a given set of flow parameters, the water signal was monitored at 20 amu ($H_2{}^{18}O^+$) while the injector was moved upward. Even at high flow velocities, the water signal was constant (± 3%) after the injector had passed the bottom 4 cm of the reactive surface, i.e., equilibrium of the carrier gas with the vapor pressure of the film was reached. The Reynold's number for a mixture of 5 Torr H_2O with 15 Torr He was calculated according to Utter et al.[20] Depending on flow velocity, it varied from 2.5 to 25, so that a laminar gas flow can be assumed.

2.5. Measurement Procedure. By translating the injector, the loss of $ClNO_2$ and the formation of products at different gas−liquid contact times was recorded. The pseudo first-order rate coefficient k_w was calculated from the variation of signal with injector position according to eq 3:

$$[ClNO_2]_{z_2} = [ClNO_2]_{z_1} \exp\left(-k_w \frac{\Delta z}{c}\right) \tag{3}$$

where $[ClNO_2]_{z_{1,2}}$ are the $ClNO_2$ concentrations at injector positions z_1 and z_2, Δz represents the distance between the positions z_1 and z_2, and c is the gas flow velocity in the tube. The ratio $\Delta z/c$ thus defines the gas−liquid contact time. At a gas flow velocity of 50 cm s^{-1} and low uptake rates, the plug flow approximation fully applies.[22] Therefore, further corrections of k_w for radial concentration gradients were not necessary and the experimental uptake coefficient γ_{expt} was obtained directly from k_w:[23]

$$\gamma_{expt} = \frac{2rk_w}{\omega} \tag{4}$$

where r is the radius of the tube and ω is the average molecular velocity of the trace gas. The resulting γ_{expt} is a representation of the overall efficiency of gas−liquid collisions to remove molecules from the gas phase.

3. Results and Discussion

3.1. Data Analysis. As discussed in detail by Davidovits et al.,[24] the overall uptake (γ_{expt}) of gas molecules into a liquid can be considered as a sequence of resistances, i.e., transport to the interface (γ_{diff}), mass accommodation (α), liquid-phase reaction (γ_{rxn}), and/or solvation (γ_{sol}) of the trace gas:

$$\frac{1}{\gamma_{expt}} = \frac{1}{\gamma_{diff}} + \frac{1}{\alpha} + \frac{1}{\gamma_{sol} + \gamma_{rxn}} \tag{5}$$

where the mass accommodation coefficient α represents the fraction of molecules that penetrate into the bulk of the liquid upon striking the surface, i.e., the probability for a molecule to cross the interface.

If experimental parameters are chosen such that one of these terms becomes rate limiting for the uptake, γ_{expt} can be approximated by relatively simple analytic expressions. In the case of diffusive limitation, $\gamma_{expt} \approx \gamma_{diff}$ applies and, corrected for a cylindrical flow tube geometry, is given by eq 6:[25]

$$\gamma_{diff} \approx \frac{3.66(2D_g)}{\omega r} \tag{6}$$

where D_g is the overall gas-phase diffusion coefficient at the pressure of the experiment. The geometry-dependent factor 3.66 is valid when axial diffusion can be neglected, i.e., if the flow velocity is much greater than the axial diffusion velocity. This condition is true when the Peclet number[26] ($2rc/D_g$) is greater than approximately 10. Peclet numbers between 30 and 70 were characteristic of the conditions used in section 3.2.

Similar terms can be derived for solubility or reaction limited uptake processes:[19,27]

$$\gamma_{sol} = \frac{4HRT}{\omega\sqrt{\pi}} \sqrt{\frac{D_l}{t}} \tag{7}$$

$$\gamma_{rxn} = \frac{4HRT}{\omega} \sqrt{D_l \sum k_{rxn}} \tag{8}$$

In these equations, H denotes the Henry's law coefficient, R is the gas constant, T is the temperature, t is the time for which the liquid is in contact with the gas, D_l is the liquid-phase diffusion coefficient, and k_{rxn} the pseudo first-order rate coefficient for a reaction of the gas with water or any other reactant present in solution in excess concentration.

3.2. Diffusion Coefficient Measurements. If loss rates of a trace gas to the liquid are high enough, i.e., γ_{expt} in the order of $(2-4) \times 10^{-3}$ for $ClNO_2$ in 10−20 Torr He as a carrier gas, gas-phase diffusion becomes the limiting parameter in kinetic measurements. By rearranging eqs 5 and 6, it can be shown that γ_{expt} is inversely proportional to the pressure of the carrier gas in this regime:

$$\frac{1}{\gamma_{expt}} = \frac{1}{\alpha} + \frac{\omega r p_{H_2O}}{7.32 D_{H_2O}^{ClNO_2}} + \frac{\omega r}{7.32 D_{He}^{ClNO_2}} p_{He} \tag{9}$$

where $D_{H_2O}^{ClNO_2}$ and $D_{He}^{ClNO_2}$ are the pressure-independent diffusion coefficient of $ClNO_2$ in water and helium, respectively, and p is the partial pressure of these gases. The overall diffusion coefficient D_{tot} (in cm^2 s^{-1}) is calculated as:

$$\frac{1}{D_{tot}^{ClNO_2}} = \frac{p_{H_2O}}{D_{H_2O}^{ClNO_2}} + \frac{p_{He}}{D_{He}^{ClNO_2}} \tag{10}$$

As uptake coefficients for $ClNO_2$ in aqueous Br^- solutions are small, NaBr was replaced by 0.1 or 0.5 M KOH to increase the uptake above the critical value for diffusion limitation. Figure 2 shows the resulting exponential $ClNO_2$ decays at different He pressures. The good linearity of the plots over a range of pressures provides some confirmation that the uptake was controlled by gas-phase diffusion. The slopes of the exponential fits yield k_w and thus define γ_{expt} (eq 4). k_w was found to be independent of either gas or liquid flow rates.

The pressures in this plot correspond to the average value of p along the flow tube, the difference between top and bottom of the reactor was typically around 0.2 Torr. In Figure 3, $1/\gamma_{expt}$ is plotted versus the carrier gas pressure for experiments in He and N_2. The pressure-independent diffusion coefficient of $ClNO_2$ in these gases can be calculated from the slope of the fit to the data as described by eq 9. Results are 275 ± 26 Torr cm^2 s^{-1} for He and 75 ± 6 Torr cm^2 s^{-1} for N_2 (errors are 95% confidence limits).

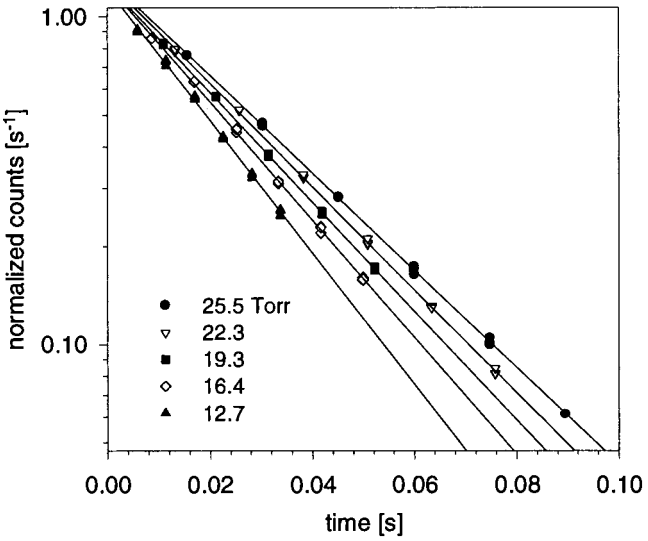

Figure 2. Decay of $ClNO_2$ during uptake onto an aqueous film containing 0.1 M KOH. The carrier gas was He, typical initial $ClNO_2$ concentrations were $\approx 2 \times 10^{14}$ cm^{-3}. The slopes of the fits yield the rate coefficient k_w for the loss of $ClNO_2$ to the liquid film.

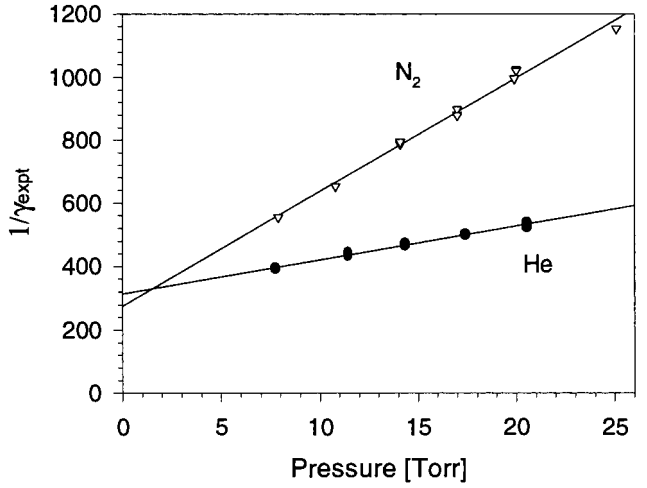

Figure 3. γ^{-1} as a function of pressure of the He or N_2 carrier gas for diffusion-limited uptake. The flow velocity was varied between 1.5 and 5 m/s, and the vapor pressure of water was held constant at 4.9 ± 0.2 Torr. Pressure-independent diffusion coefficients for $ClNO_2$ in He and N_2 were found to be 275 ± 26 and 75 ± 6 Torr cm^2 s^{-1}, respectively.

Also from eq 9, it is evident that the *y*-axis intercept of the fit contains information about α and $D_{H_2O}^{ClNO_2}$. The relation between both parameters is given by:

$$D_{H_2O}^{ClNO_2} = \frac{\omega r p_{H_2O}}{7.32\left(y_0 - \frac{1}{\alpha}\right)} \qquad (11)$$

where y_0 denotes the intercept of the lines in Figure 3 with the *y*-axis.

By making a reasonable estimation of $D_{H_2O}^{ClNO_2}$, eq 11 allows α to be estimated. By analogy with the diffusion coefficients of N_2, CO_2,[28] and NO_3[29] in helium and water vapor, we calculate a value of 2.75 ± 0.25 for the ratio D_{He}/D_{H_2O}. Using our value of = 275 ± 26 Torr cm^2 s^{-1}, we calculate 100 ± 20 Torr cm^2 s^{-1}, and therefore $\alpha = (9 \pm 4) \times 10^{-3}$.

3.3. Uptake of $ClNO_2$ on Br^- Solutions. Both kinetic (γ) and mechanistic information was obtained for the uptake of

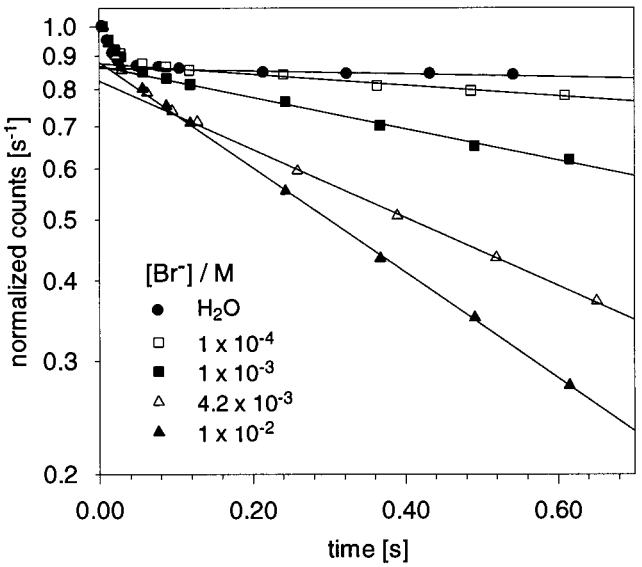

Figure 4. Decay of $ClNO_2$ during uptake onto H_2O and aqueous Br^- films. The initial $ClNO_2$ concentration was $\approx 2 \times 10^{14}$ cm^{-3}. The slopes of the fits (to exponential part of decay only) yield directly the first-order rate coefficient k_w for the loss of $ClNO_2$ to the liquid film.

$ClNO_2$ onto solutions of different Br^- content according to the following reactions:

$$ClNO_2 + H_2O \rightarrow 2\,H^+ + NO_3^- + Cl^- \qquad (R4)$$

$$ClNO_2 + Br^- \rightarrow \text{products} \qquad (R5)$$

Figure 4 displays the decay of $ClNO_2$ during uptake onto solutions containing various Br^- concentrations. Variation of the initial $ClNO_2$ concentration in the range $2-5 \times 10^{14}$ cm^{-3} had no effect on the uptake rates. The exponential decay of $ClNO_2$ at contact times between 0.1 and 0.7 s on all solutions used indicates that in this time period the experimentally observed uptake is influenced neither by the loss of Br^- in the film nor by the solubility of the reactant. Therefore, γ_{expt} is described by:

$$\frac{1}{\gamma_{expt}} = \frac{1}{\alpha} + \frac{\omega}{4RT}\frac{1}{H\sqrt{D_1(k_{H_2O}^I + k_{Br}^{II}[Br^-])}} \qquad (12)$$

where $k_{H_2O}^I$ is the rate coefficient for hydrolysis of $ClNO_2$, and k_{Br}^{II} is the rate coefficient for the reaction with Br^-. As discussed previously, a lower limit of $\alpha = 5 \times 10^{-3}$ can be estimated. If we rewrite eq 12 without considering the influence of α (eq 13), a maximum error of 2% for the single γ-values is introduced. Thus, to a good approximation:

$$\gamma_{expt}^2 = \left(\frac{4RT}{\omega}\right)^2 H^2 D_1(k_{H_2O}^I + k_{Br}^{II}[Br^-]) \qquad (13)$$

When γ_{expt}^2 is plotted vs the Br^- concentration (Figure 5), $H^2D_1k_{Br}^{II}$ can be calculated from the slope of the resulting line as (0.101 ± 0.015) M cm^2 atm^{-2} s^{-2}. Its intercept with the *y*-axis defines $H^2D_1k_{H_2O}^I$ as $5.8^{+12}_{-5} \times 10^{-7}$ M^2 cm^2 atm^{-2} s^{-2}.

In Table 1 we compare our results to very recently obtained data for $ClNO_2$ uptake onto Br^- solutions. Frenzel et al.[30] used a high-pressure (760 Torr) wetted wall reactor at 2 °C with matrix-isolation-FTIR detection of $ClNO_2$, whereas Schweizer et al.[31] used a wetted wall flow reactor at pressures similar to

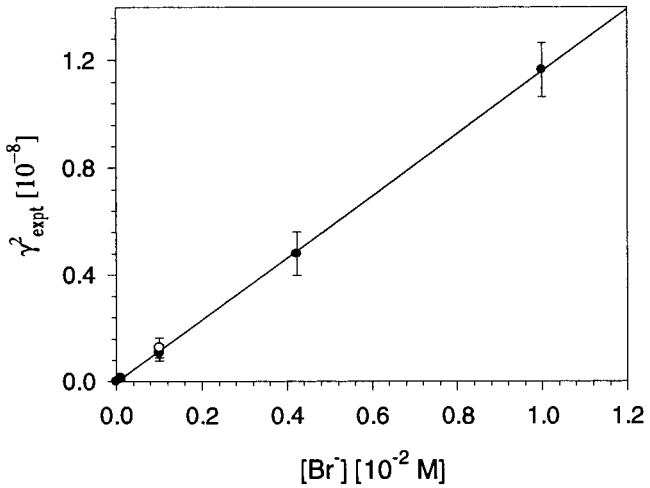

Figure 5. Plot of γ^2 vs Br^- concentration for the uptake of $ClNO_2$ on pure Br^- (filled symbols) and a mixed Br^-/Cl^- solution (1 M Cl^-, open symbol). From the slope of the fit (see eq 13) a value of $H^2D_l k_{Br} = (0.101 \pm 0.015)$ M cm^2 atm^{-2} s^{-2} could be obtained.

TABLE 1: Uptake Coefficients for $ClNO_2$ on Br^- Solutions[a]

Br^- [M]	$10^6\,\gamma$ (this work)	$10^6\,\gamma$ (ref 30)[b]	$10^6\,\gamma$ (ref 31)[c]
0	2.6 ± 1.8		
1×10^{-4}	11.2 ± 3.9		7.1 ± 1.9
5×10^{-4}		12.5 ± 2.5	
1×10^{-3}	32.9 ± 5.0	14.6 ± 1.5	26.0 ± 7.9
4.2×10^{-3}	69.7 ± 5.6		
5.0×10^{-3}		40.2^{+16}_{-3}	
1×10^{-2}	108.6 ± 4.6		80.7 ± 7.8
1×10^{-1}			400 ± 7
1			919 ± 78
1×10^{-3} + 1 M Cl^-	35.6 ± 5.0		

[a] This work: data obtained at helium pressures between 14 and 18 Torr and a temperature of 274 K. The mixed Br^-/Cl^- solution corresponds approximately to the average composition of sea water, errors are 2 σ. [b] Ref 30: Data obtained at 760 Torr and 275 K. [c] Ref 31: Data obtained at 275 K and pressures of between 15 and 30 Torr.

the present experiments. The present data and those of Schweizer et al. appear to be in reasonable agreement.

The nonexponential and rapid decay of $ClNO_2$ at $t < 0.1$ s is not due to incomplete mixing of the injector gas with the main flow before sampling into the mass spectrometer as the two flows are thoroughly mixed downstream of the wetted wall region. Also, this effect was observed in experiments on pure water and is therefore not caused by the evaporation of H_2O from the aqueous film just past the injector that might result in a more concentrated Br^- surface layer and more rapid uptake. As discussed later, we observe no product formation during this initial uptake period, which is probably due to nonreactive uptake of $ClNO_2$, i.e., solvation.

3.4. Product Studies. As shown by our uptake experiments, the loss of $ClNO_2$ in Br^- solutions of atmospheric relevance ($[Br^-] \geq 10^{-4}$ M, $[Cl] \geq 1$ M) proceeds predominantly via reaction with Br^-, as hydrolysis is too slow to compete. As discussed by Frenzel et al.[32] the following reactions may be considered to contribute to the loss of $ClNO_2$:

$$ClNO_2 + Br^- \rightarrow BrCl + NO_2^- \qquad (R5a)$$

$$ClNO_2 + Br^- \rightarrow BrNO_2 + Cl^- \qquad (R5b)$$

BrCl and $BrNO_2$ are expected to undergo subsequent reactions with Br^- to form Br_2:

$$BrCl + Br^- \rightleftarrows Br_2Cl^- \qquad (R 6, R -6)$$

$$Br_2Cl^- \rightleftarrows Br_2 + Cl^- \qquad (R 7, R -7)$$

$$BrNO_2 + Br^- \rightleftarrows Br_2 + NO_2^- \qquad (R 8, R -8)$$

Both the decay of $ClNO_2$ and the products of its reaction with Br^-, (Br_2, $BrNO_2$, and BrCl) were recorded. As the $ClNO_2$ samples contained 1−3% Cl_2 impurity, which results in BrCl formation when taken up onto Br^- solutions, additional Cl_2 uptake experiments were carried out under otherwise identical conditions in order to correct the BrCl profiles. To check for a possible influence of the surface depletion of Br^- at low ion concentrations, the initial concentrations of $ClNO_2$ were reduced by 50%. This had no discernible effect on the product yields.

The mass spectrometer was calibrated for Cl_2, Br_2, and BrCl by introducing a defined flux of these gases into the reactor, and for $ClNO_2$ by calculating its flow rate into the flow tube from a pressure drop in a defined volume. For $BrNO_2$, an indirect calibration method was chosen, which required ion chromatographic analysis of the liquid phase. Although a method to synthesize $BrNO_2$ has been developed[32] accurate vapor pressures are unavailable and so a well-defined flow rate of nitryl bromide into the reactor could not be realized. Instead, $BrNO_2$ was produced in situ by reacting Br_2 (ca. 1×10^{13} cm^{-3}) on a liquid film containing 10^{-4} M NO_2^- (R −8), as described by Frenzel et al.[30] Using ion chromatography to analyze the liquid phase it could be shown that the loss of Br_2 from the gas phase results in an equivalent loss of NO_2^- from the film when the ratio of liquid flux/gas flux is taken into account. Thus, $BrNO_2$ was calibrated by equating the amount of NO_2^- lost from the liquid to the counts at 93 amu. As a possible source of error, the reaction

$$BrNO_2 + NO_2^- \rightarrow Br^- + N_2O_4 \qquad (R 9)$$

has to be considered. If N_2O_4 was produced, it would be released to the gas phase ($H = 1.4$ M atm^{-1}).[33] Consequently, additional NO_2^+ fragments, not originating from the fragmentation of $BrNO_2$, would be formed and the ratio BrN^+/NO_2^+ in the MS would change. To test for this, experiments were carried out in which the ratio of $BrNO_2$(g) to NO_2^-(liq) was varied by 2 orders of magnitude. The amount of NO_2^- lost from the liquid phase varied between <5% and 40%. No change in the BrN^+/NO_2^+ signal ratio was observed, and we conclude that reaction 9 is unimportant. To estimate the influence of physical solubility of $BrNO_2$ on the calibration, a numerical simulation[34] of the gas- and liquid-phase diffusion of all reactants, the phase transfer, and the liquid-phase reactions was undertaken. The simulation calculates concentration−time profiles for a static system, i.e., the relative velocities of the gas and the liquid phase are neglected. Results indicate that the amount of $BrNO_2$ remaining in the liquid is less than 1% of the total $BrNO_2$ produced, even with Henry's law coefficients as high as 1 M atm^{-1}. Finally, the reaction of $BrNO_2$ with Br^- (R 8) does not introduce an error to our calibration, as it reforms Br_2 and thus cancels in the overall balance.

Typical concentration−time profiles for the formation of products following the uptake of $ClNO_2$ on two solutions of different Br^- concentration are shown in Figure 6. The relative concentrations of the Br_2 and $BrNO_2$ products are clearly shifted toward Br_2 as the Br^- content of the solution is increased, and

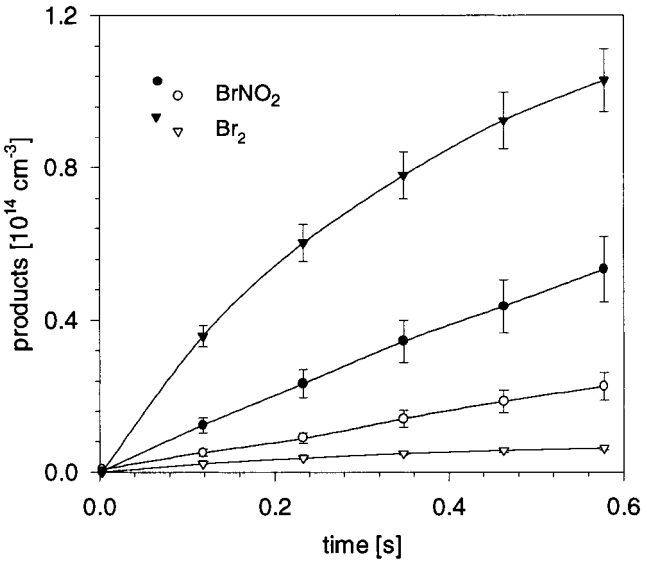

Figure 6. Gas-phase products from the reaction of $ClNO_2$ on 10^{-4} M Br^- solutions (open symbols) and 4.2×10^{-3} M solutions (filled symbols) versus time. The overall increase in product formation at high concentrations reflects the enhanced uptake of $ClNO_2$ under these conditions. The initial $ClNO_2$ concentration was in both cases 5×10^{14} cm^{-3}. Within error, the product distribution remained unaffected by the addition of 1 M Cl^- to the liquid film.

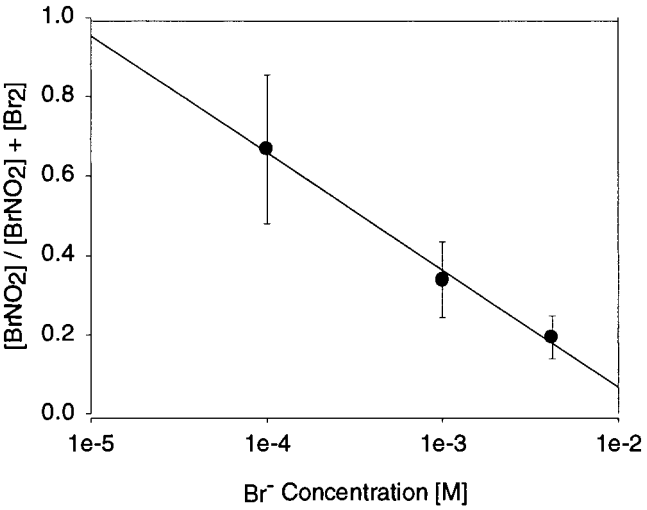

Figure 7. Partitioning of the brominated gas-phase products ($BrNO_2$, Br_2) at different Br^- concentrations, following correction for uptake of Br_2 and conversion to $BrNO_2$ (see text for details).

the total amount of gas-phase products increases substantially. This is consistent with the results of Frenzel et al.[30] who observed rapid uptake of $BrNO_2$ onto NaBr solutions and formation of Br_2. In Figure 7, the ratio of $BrNO_2$ to the total amount of brominated species formed ($BrNO_2 + Br_2 + BrCl = BrX$) is plotted against [$Br^-$]. At low [$Br^-$], $BrNO_2$ is the dominant gas-phase product following uptake and reaction of $ClNO_2$. Although BrCl was detected, its concentration was always more than 2 orders of magnitude lower than those of the main products, Br_2 and $BrNO_2$. The total yields of gas-phase products relative to the loss of $ClNO_2$ from the gas phase (Figure 8) enables the efficiency of $ClNO_2$ to activate bromine species to be estimated. The efficiency, $\Delta BrX/\Delta ClNO_2$, determined from the slope of the data in Figure 8, was found to be $70 \pm 18\%$, independent of the amount of Br^- present in solution within the range studied. Reduction of the absolute concentration of $ClNO_2$ from $\approx 5 \times 10^{14}$ (Figure 8, filled symbols) to 2×10^{14} cm^{-3} (Figure 8, open symbols) resulted in a proportional

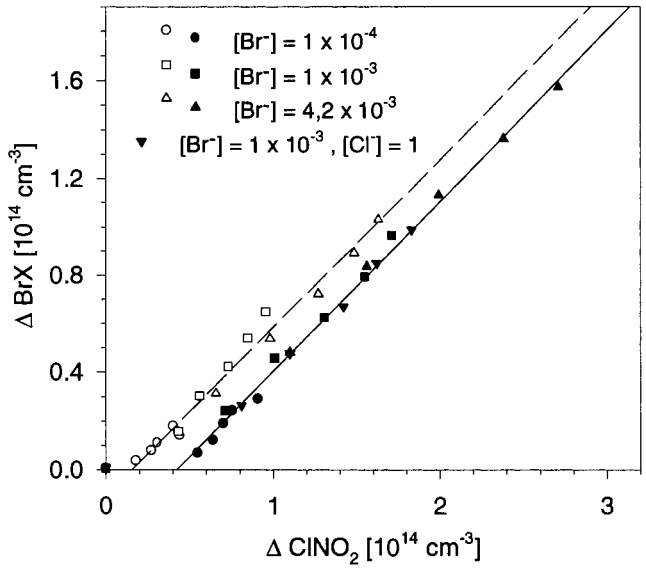

Figure 8. Sum of $BrNO_2$ and Br_2 plotted vs the amount of $ClNO_2$ lost on Br^- and synthetic sea-salt solutions ([Br^-] = 10^{-3} M, [Cl^-] = 1 M). An amount of $70 \pm 18\%$ of the $ClNO_2$ taken up was released as bromine-containing species, independent of Br^- concentration. Filled symbols, $[ClNO_2]_0 = 5 \times 10^{14}$ cm^{-3}; open symbols, $[ClNO_2]_0 = 2 \times 10^{14}$ cm^{-3}.

decrease of the offset on the $\Delta ClNO_2$ axis, while the slope of the fit to the data remained unchanged. The *x*-axis offset in both data sets of Figure 8 is due to an enhanced (but nonreactive) uptake of the reactant within the first few milliseconds of interaction. As the size of the offset is proportional to the absolute amount of $ClNO_2$ present in the gas phase, this effect is probably related to the physical solubility of the reactant.

Recently, mechanisms for the reaction of $ClNO_2$ with nucleophiles such as OH^-, I^- or Cl^- have been discussed in the literature.[6,35,36] $BrNO_2$ may be produced either directly from $ClNO_2$ by nucleophilic substitution (R 5b) or via the dissociative formation of a nitronium ion (R 10, R 11).

$$ClNO_2 + Br^- \rightarrow BrNO_2 + Cl^- \qquad \text{(R 5b)}$$

$$ClNO_2 \rightleftarrows Cl^- + NO_2^+ \qquad \text{(R 10, R } -10\text{)}$$

$$NO_2^+ + Br^- \rightarrow BrNO_2 \qquad \text{(R 11)}$$

The dissociation (R 10) was shown to be reversible in studies of the uptake of N_2O_5 on Cl^- solutions.[6] As the product yields and distribution in our experiments on 10^{-3} M Br^- solutions were not affected by the addition of 1 M Cl^- to the liquid (Figure 8), we can draw a lower limit for the ratio k_{5b}/k_{12} of $\approx 1 \times 10^4$.

$$ClNO_2 + Cl^- \rightarrow \text{products} \qquad \text{(R 12)}$$

Previous studies on the reaction of N_2O_5 on mixed Br^-/Cl^- solutions[6] have yielded values of $k_{11}/k_{-10} < 10^3$. Given this, a reaction of NO_2^+ with Cl^- would be expected to perturb our Br_2 and $BrNO_2$ product yields in experiments with 1M Cl^- and 1×10^{-3} M Br^- if formation of NO_2^+ (R 10) were the first step in the reaction of $ClNO_2$ with the halide solutions. This was not observed, and we conclude the direct formation of $BrNO_2$ (R 5b) takes place in our experiment. This conclusion is also supported by the observation of much slower uptake of $ClNO_2$ onto H_2O compared with 1×10^{-3} M bromide solutions (see Table 1).

As the sum of all BrX (X = Br, NO_2) released to the gas phase is constant, while the relative concentrations of $BrNO_2$ and Br_2 are shifted toward Br_2 with increasing Br^- content of the solution, we can assume that $BrNO_2$ is an intermediate product which reacts further to form Br_2:

$$BrNO_2 + Br^- \rightarrow Br_2 + NO_2^- \qquad \text{(R 8)}$$

If the ratio $BrNO_2$/BrX is plotted vs the Br^- concentration, the intercept at $[Br^-] = 0$ should yield the fraction of $BrNO_2$ that is unaffected by R 8. Figure 7 shows that initial formation of $BrNO_2$ is responsible for up to 100% (± 30%) of the total BrX production in these experiments. To correct for the fact that Br_2 concentrations in the gas phase, as well as NO_2^- concentrations in the film increased with increasing contact time, which may result in $BrNO_2$ formation (R −8), the $BrNO_2$/BrX values were corrected by extrapolating the ratio $BrNO_2$/BrX at a given Br^- concentration to $t = 0$ s. That is, from the data in Figure 6, the ratio $[BrNO_2]/([Br_2]+ [BrNO_2])$ increases from 0.205 at $t = 118$ ms, to 0.25 at $t = 578$ ms for 4×10^{-3} M Br^- solution. For $[Br^-] = 10^{-4}$ M, these values were 0.696 at 118 ms, and 0.790 at 578 ms.

The results discussed above leave room for another mechanism for Br_2 formation. As we detect BrCl in amounts of $(1-5) \times 10^{11}$ cm^{-3}, reactions 6 and 7 have to be considered. According to Wang et al.[37] the fast equilibrium between reactions 6,−6, 7, and −7 can lead to Br_2 production rather than the release of BrCl from Br^- solutions. However, in separate experiments on the uptake of HOBr onto Cl^--containing solutions we have observed high yields of BrCl (25% BrCl and 75% Br_2) per HOBr taken up in the presence of 1×10^{-4} M Br^-. We therefore conclude that a significant proportion of any BrCl formed in the present experiments in reaction 5a would be released from the liquid phase and detected. As only minor (<1%) amounts of BrCl relative to $BrNO_2$ and Br_2 were detected, we rule out an important role for BrCl formation in the present experiments and conclude that reactions 5b and 8 are sufficient to explain the observed Br_2 production. These results are entirely consistent with conclusions drawn from uptake measurements of $ClNO_2$ and $BrNO_2$ on dry bromide salts.[38] In addition, we note that Cl_2 was not observed as a product (upper limit of < 1% $Br_2/BrNO_2$ yield) when uptake experiments on solutions of 1 M $Cl^- + 1 \times 10^{-3}$ M Br^- were carried out.

Our proposed overall mechanism to the observed gas-phase products is shown in Figure 9. We note that this scheme does not fully describe the fate of $ClNO_2$ in a Br^- solution, as the sum of all observed products amounts to a maximum of 88% of the $ClNO_2$ taken up.

To roughly estimate the fate of $ClNO_2$ in the marine boundary layer an analytical model of trace gas−aerosol interaction was adopted.[39] With a Br^- concentration of 10^{-3} M and a liquid-phase diffusion coefficient of ca. 10^{-5} cm^2 s^{-1} in aerosol droplets of radius 1×10^{-4} cm, the uptake of $ClNO_2$ is limited by liquid-phase processes. That is, its rate of removal depends on the Henry's law coefficient H and k^I, the first-order loss rate coefficient,[40] which were determined interdependently as $H^2k \approx 10$ M^2 atm^{-2} s^{-2}. With an assumed lower limit of H of 0.1 M atm^{-1} and for a typical liquid water content in the aerosol of 7×10^{-11} (cm^3/cm^3), a lifetime of $ClNO_2$ due to uptake of ca. $10^6 - 10^7$ s (≈10−100 days) can be estimated. This value has to be compared to an average photolytic lifetime of ca. 3×10^3 s (<1 h) at a solar zenith angle of 45°.[41] In conclusion, we find that $ClNO_2$, once released to the marine troposphere, can be considered as a source of atomic Cl through photolysis at mid-latitudes. Only during polar winter where the marine boundary layer is in total darkness for several months prior to sunrise, can heterogeneous processing of $ClNO_2$ take place. The rate of formation of gas-phase Br-containing species via heterogeneous conversion of N_2O_5 to $ClNO_2$ and the subsequent uptake of $ClNO_2$ and release of Br_2 (and $BrNO_2$) will probably be limited by the availability of NO_x in this environment.

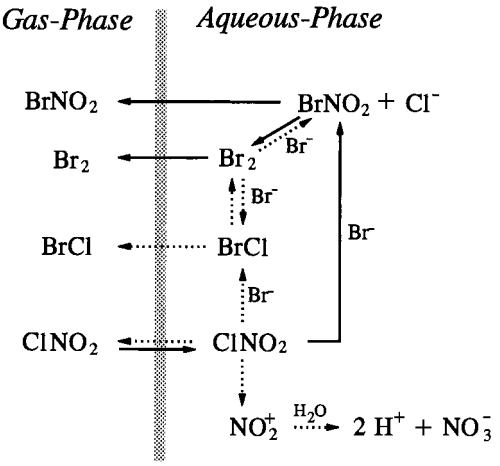

Figure 9. Possible pathways for reactions of $ClNO_2$ in aqueous Br^- solutions. The solid lines are the major pathways in the present experiments. Dotted lines represent minor pathways.

3.5. Conclusions. The uptake coefficients of $ClNO_2$ on Br^- solutions range from $\gamma \approx 1 \times 10^{-5}$ to 1×10^{-4} at Br^- concentrations of $10^{-4} - 10^{-2}$ M. The accommodation coefficient at 274 K was determined as $(9 \pm 4) \times 10^{-3}$. The diffusion coefficients of $ClNO_2$ were determined in both He and N_2 bath gases as 275 ± 26 Torr cm^2 s^{-1} and 75 ± 6 Torr cm^2 s^{-1}, respectively. By determining γ as a function of Br^-, a value for $H^2D_1k_{Br}^{II}$ of 0.101 ± 0.015 M cm^2 $Torr^{-2}$ s^{-2} was obtained. For the first time, the gas-phase products of the reaction of $ClNO_2$ with Br^-, (BrCl, Br_2, and $BrNO_2$), were recorded simultaneously and quantified, showing that $ClNO_2$ taken up on sea-salt type liquids is converted to Br-containing species at a significant percentage. The major gas-phase, bromine-containing product following $ClNO_2$ uptake onto atmospheric sea-salt aerosol ($[Br^-] > 1 \times 10^{-3}$ M) is Br_2.

Acknowledgment. The authors thank Dr. Shaun Carl for help with the UV-absorption measurements of BrCl, and Dr. Michel Rossi for making his results available prior to publication. This work was supported by the European Union (SALT, ENV4-CT95-0037).

References and Notes

(1) Pszenny, A. A. P.; Keene, W. C.; Jacob, D. J.; Fan, S.; Maben, J. R.; Zetwo, M. P.; Springer-Young, M.; Galloway, J. N. *Geophys. Res. Lett.* **1993**, *20*, 699.

(2) Wingenter, O. W.; Kubo, M. K.; Blake, N. J.; Smith, T. W., Jr.; Blake, D. R.; Rowland, F. S. *J. Geophys. Res.* **1996**, *101*, 4331.

(3) Singh, H. B.; Gregory, G. L.; Anderson, B.; Browell, E.; Sachse, G. W.; Davis, D. D.; Crawford, J.; Bradshaw, J. D.; Talbot, R.; Blake, D. R.; Thornton, D.; Newell, R.; Merrill, J. *J. Geophys. Res.* **1996**, *101*, 1907.

(4) Martens, C. S.; Wesolowski, J. J.; Harriss, R. C.; Kaifer, R. *J. Geophys. Res.* **1973**, *78*, 8778.

(5) Finlayson-Pitts, B. J.; Ezell, M. J.; Pitts, J. N., Jr. *Nature* **1989**, *337*, 241.

(6) Behnke, W.; George, C.; Scheer, V.; Zetzsch, C. *J. Geophys. Res.* **1997**, *102*, 3795, (and references therein).

(7) Jobson, B. T.; Niki, H.; Yokouchi, Y.; Bottenheim, J.; Hopper, F.; Leaitch, R. *J. Geophys. Res.* **1994**, *99*, 25355.

(8) Ramacher, B.; Rudolph, J.; Koppmann, R. *Tellus* **1997**, *49B*, 466.

(9) Hausmann, M.; Platt, U. *J. Geophys. Res.* **1994**, *99*, 25399.

(10) Tuckermann, M.; Ackermann, R.; Gölz, C.; Lorenzen-Schmidt, H.; Senne, T.; Stutz, J.; Trost, B.; Unold, W.; Platt, U. *Tellus* **1997**, *49B*, 533.
(11) Martinez, M.; Arnold, T.; Seuwen, R.; Perner, D. *Geophys. Anal*., submitted 1998.
(12) McConnell, J. C.; Henderson, G. S.; Barrie, L.; Bottenheim, J.; Niki, H.; Langford, C. H.; Templeton, E. M. J. *Nature* **1992**, *355*, 150.
(13) Mozurkewich, M. *J. Geophys. Res.* **1995**, *100*, 14199.
(14) Tang, T.; McConnell, J. C. *Geophys. Res. Lett.* **1996**, *23*, 2633.
(15) Fan, S.-M.; Jacob, D. J. *Nature* **1992**, *359*, 522.
(16) Fenter, F. F.; Caloz, F.; Rossi, M. J. *J. Phys. Chem.* **1996**, *100*, 1008.
(17) Maric, D.; Burrows, J. P.; Moortgat, G. K. *J. Photochem. Photobiol. A: Chem.* **1994,** *83*, 179.
(18) Volpe, M.; Johnston, H. S. *J. Am. Chem. Soc.* **1956**, *78*, 3903.
(19) Danckwerts, P. V. *Gas*−*liquid reactions*; McGraw-Hill: New York, 1970.
(20) Utter, R. G.; Burkholder, J. B.; Howard, C. J.; Ravishankara, A. R. *J. Phys. Chem.* **1992**, *96*, 4973.
(21) Pruppacher, H. R.; Klett, J. D. *Microphysics of clouds and precipitation*; Reidel: Dordrecht, 1978.
(22) Brown, R. L. *J. Res. Natl. Bur. Stand. (U.S.)* **1978**, *83*, 1.
(23) Howard, C. J. *J. Phys. Chem.* **1979**, *83*, 3.
(24) Davidovits, P.; Hu, J. H.; Worsnop, D. R.; Zahniser, M. S.; Kolb, C. E. *Faraday Discuss.* **1995**, *100*, 65.
(25) Hanson, D. R.; Burkholder, J. B.; Howard, C. J.; Ravishankara, A. R. *J. Phys. Chem.* **1992**, *96*, 4979.
(26) Murphy, D. M.; Fahey, D. W. *Anal. Chem.* **1987**, *59*, 2753.
(27) Jayne, J. T.; Duan, S. X.; Davidovits, P.; Worsnop, D. R.; Zahniser, M. S.; Kolb, C. E. *J. Phys. Chem.* **1991**, *95*, 6329.
(28) *Handbook of Chemistry and Physics*; Lide, D. R., Ed.; CRC Press: Boca Raton, 1997.
(29) Rudich, Y.; Talukdar, R. K.; Ravishankara, A. R.; Fox, R. W. *J. Geophys. Res.* **1996**, *101*, 21023.
(30) Frenzel, A.; Scheer, V.; Sikorski, R.; George, C.; Behnke, W.; Zetzsch, C. *J. Phys. Chem.* **1998**, *102*, 1329.
(31) Schweizer, F.; Mirabel, P.; George, C. *J. Phys. Chem.* **1998**, *102*, 3942.
(32) Frenzel, A.; Scheer, V.; Behnke, W.; Zetzsch, C. *J. Phys. Chem.* **1996**, *100*, 16447.
(33) Schwartz, S. E.; White, W. H. Solubility equilibria of the nitrogen oxides and oxyacids in dilute aqueous solutions. In *Advances in Environmental Sciences and Engineering*; Pfaflin, J. R., Ziegler, E. N., Eds.; Gordon and Breach Science Publishers: New York, 1981; Vol. 4, pp 1−45.
(34) Curtis, A. R.; Sweetenham, W. P. *Facsimile Program*. AERE Report R-12805, HMSO, London, 1987.
(35) Johnson, D. W.; Margerum, D. W. *Inorganic Chemistry* **1991**, *30*, 4845.
(36) George, C.; Behnke, W.; Scheer, V.; Zetzsch, C.; Magi, L.; Ponche, J. L.; Mirabel, P. *Geophys. Res. Lett.* **1995**, *22*, 1505.
(37) Wang, T. X.; Kelley, M. D.; Cooper, J. N.; Beckwith, R. C.; Margerum, D. W. *Inorg. Chem.* **1994**, *33*, 5872.
(38) Caloz, F.; Seisel, S.; Fenter, F. F.; Rossi, M. J. *J. Phys. Chem.* **1998**, *102*, 7470.
(39) Schwartz, S. E. Mass-transport considerations pertinent to aqueous phase reactions of gases in liquid water clouds. In *Chemistry of Multiphase Systems*; Jaeschke, W., Ed.; 1986.
(40) Hanson, D. R.; Ravishankara, A. R.; Solomon, S. *J. Geophys. Res.* **1994**, *99*, 3615.
(41) Ganske, J. A.; Berko, H. N.; Finlayson-Pitts, B. J. *J. Geophys. Res.* **1992**, *97*, 7651.